MEASUREMENTS OF LONGITUDINAL WAKEFIELDS IN THE SLC COLLIDER ARCS*

K.L.F. Bane, P. Emma, M.G. Minty, F. Zimmermann
Stanford Linear Accelerator Center, Stanford, CA 94309

Abstract

We report measurements of the profile of the wakefield-induced energy loss of the beam along the 1.2 km long SLC North Collider Arc. By measuring orbit differences in dispersive regions for different bunch lengths, the wakefield-generated energy loss is distinguished from losses due to synchrotron radiation. Calculations of the wakefields arising in the arc chambers are given and used in simulations of the evolution of the longitudinal phase space along the arcs. The measurements are consistent with the calculations. By this method wakefield anomalies in the arcs can be found. In addition, with a non-standard setting of parameters the bunch can be compressed down to ~ 50 μm, and the wakefield effect of an ultra-short bunch can be observed. Results for the final focus wakefield-induced losses are also given.

1 INTRODUCTION

In the Stanford Linear Collider (SLC) after leaving the damping ring, the beam is compressed in the Ring-to-Linac (RTL) transfer line, accelerated in the linac, and transported through the 1.2 km long arc transfer line to the final focus (FF) region and the interaction point (IP). At times, in the arcs, an unexplained emittance growth has been observed. The likely cause is a transverse wakefield effect, though verification of this idea has proven to be difficult. A longitudinal wakefield effect—the wakefield induced energy loss—on the other hand, can be measured relatively accurately, and the results can be used to test our understanding of the wakefields in the SLC arcs in general.

The wakefield-induced energy loss in the arcs depends on bunch length as an inverse power, while the (much larger) synchrotron radiation losses are independent of bunch length. Therefore, we can distinguish the wakefield effect by measuring the orbit difference in dispersive regions for different bunch length profiles. In this report we describe such measurements. The bunch length profile in the arcs is changed by varying both the peak voltage of the bunch compressor in the RTL and the phase of the beam with respect to the rf wave in the linac. One interesting feature of our measurements is that, due to the large momentum compaction factor of the arcs and a non-negligible energy spread induced in the linac, the bunch length can change dramatically during the beam's passage through the arcs. We compare the results with calculations. Finally, we repeat the process for the SLC final focus.

This study allows us to: (1) check the consistency of our wakefield model, (2) find the location of anomalous wakefield sources, and (3) study the wakefield effect for ultra-short bunches (rms length $\sigma_z \sim 50$ μm *vs* the nominal ~ 1 mm). Note that similar measurements were performed in a storage ring, at LEP[1], where the energy loss profile was determined by comparing orbits for different bunch currents, rather than for different bunch lengths.

*Work supported by the Department of Energy, contract DE-AC03-76SF00515

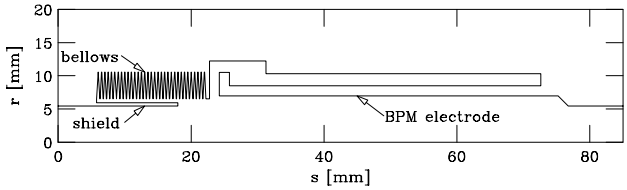

Figure 1: Longitudinal profile of a North arc BPM/bellows module, showing the bellows, the bellows shield, and the BPM. Note that the beam tube radius is at $r = a \approx 5$ mm.

2 WAKEFIELDS AND SIMULATIONS

The arc vacuum chamber is comprised of 460 evenly-spaced, BPM/bellows modules that are separated by aluminum, cylindrical beam pipe of radius $a = 5$ mm. In the North arc the bellows are partially shielded (see Fig. 1), in the South arc they are not. The arc wakefields can be thought of consisting of two parts, a resistive-wall (RW) component, due to the beam pipe, and a geometric (G) one, due to the BPM/bellows modules.

For a Gaussian bunch in a cylindrical tube the average energy change (over the bunch) due to the RW wake is[2]

$$(\Delta E)_{RW} = -\frac{\Gamma(3/4)}{4\sqrt{2}\pi^2}\frac{e^2 N L c}{a\sigma_z^{3/2}}\sqrt{\frac{Z_0}{\sigma_c}}, \qquad (1)$$

with $\Gamma(3/4) \cong 1.23$ and $Z_0 \cong 377\ \Omega$; N is the bunch population, L the tube length, and σ_c the conductance of the metal (= 36 Mmho/m for Al). To obtain the G wake contribution in the North arc the energy change, for Gaussians of different lengths, was computed for the structure shown in Fig. 1, using the computer program MAFIA [3]. Over the bunch length range [0.1 mm,2 mm] the results for each BPM/bellows module are well parameterized by

$$(\Delta E)_G / \mathrm{eV} = \left(\frac{eN}{\mathrm{pC}}\right)\left[4.5 - 8.7\left(\frac{\sigma_z}{\mathrm{mm}}\right)^{-\frac{1}{2}}\right]. \qquad (2)$$

In our calculations (as in the measurements) we take $N = 3.5\times10^{10}$. For a constant $\sigma_z = 0.5$ mm, for example, the total calculated RW and G losses in the arcs are 2.6 and 20 MeV, respectively, results which are much smaller than the loss due to synchrotron radiation, which is 1 GeV (at 46 GeV). Note that coherent synchrotron radiation for the

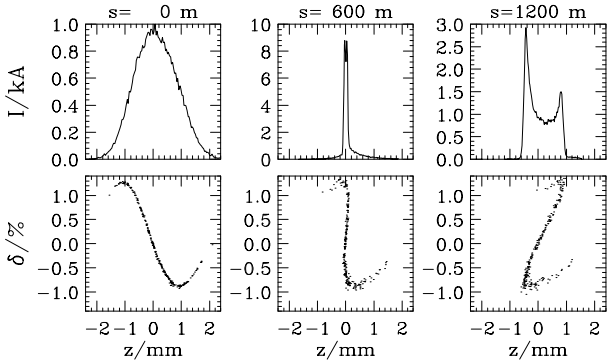

Figure 2: Simulated bunch profile (top) and longitudinal phase space (bottom) at arc entrance ($s = 0$, $\sigma_z \approx 790$ μm), arc middle ($s = 600$ m, 65 μm), and arc end ($s = 1200$ m, 570 μm), for $V_c = 37.2$ MV and $\phi = -5.6°$; z is longitudinal position in the bunch ($z < 0$ is toward the head), δ is relative energy deviation, and I is current.

arcs is effectively shielded by the vacuum chamber, even for bunch lengths as short as 25 μm rms, and this effect can be ignored.

Using a macro-particle approach the longitudinal phase space of the beam is tracked from the damping ring, through the compressor, linac, and arc to the final focus[4]. The (initial) ring position and energy distributions are those obtained by measurements (as here) at a ring rf voltage of 0.8 MV[5]. The arc compaction factor $R_{56} = 14.5$ cm. An example, with parameters corresponding to the measurements discussed below—compressor voltage $V_c = 37.2$ MV and linac phase $\phi = -5.6°$ (note: $\phi < 0$ indicates that the beam is in front of the rf crest)—and illustrating the large bunch length change that can occur in the arcs, is given in Fig. 2. Finally, during the simulations, to estimate the local arc wakefield losses, the local value of $z_{FWHM}/2.355$, with z_{FWHM} the full width of the bunch distribution, is substituted into Eqs. 1 and 2.

3 MEASUREMENTS

To obtain the wakefield induced energy loss in the arcs the orbit was measured twice, for two different bunch length profiles, and then the two orbits were subtracted. The bunch length profile was modified by changing the voltage of the bunch compressor V_c and the average linac rf phase of the beam ϕ. The former method directly changes the bunch length in the linac; the latter method changes the energy spread of the beam at the entrance to the arcs, which through the compaction factor, changes the bunch length evolution in the arcs.

Each SLC arc consists of 23 52-m long achromatic sections and has a 280-meter bend radius, which reverses direction at $s \approx 400$ m. The lattice is a FODO structure based on combined-function magnets, with 10 FODO cells per achromat and 108° betatron phase advance per cell. Near each magnet a BPM is installed for a total of 460 BPMs (230 x-BPMs and 230 y-BPMs). The average horizontal

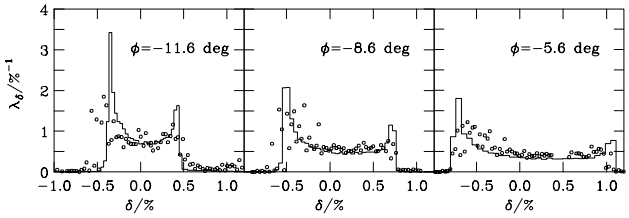

Figure 3: The beam energy distribution as measured at the end of the linac for 3 different linac phases, when $V_c = 37.2$ MV (the symbols). For comparison, simulation results are also given (the histograms).

dispersion in the arc $\langle|\eta_x|\rangle = 35$ mm; it changes sign at $s \approx 400$ m. If we measure the energy change per achromat by summing its 10 x-BPMs and average over 10 pulses, the resolution per 52-meter section is

$$\frac{\Delta E}{E} \approx \frac{\Delta x}{10\langle|\eta_x|\rangle} \approx 3 \times 10^{-5}, \qquad (3)$$

or 1.3 MeV, where we assume a BPM resolution, Δx, of 10 μm. Using the 10-BPM sum, the measurement is insensitive to betatron motion since the beta functions do not change and the summed group covers 6π in betatron phase. For short bunches, the energy loss is much larger than the resolution and therefore detectable.

At the same time of the arc orbit measurements the beam spectrum at the end of the linac was also measured, by means of a wire monitor located in a dispersive region. Since the bunch length profile along the arcs depends sensitively on the beam conditions at the entrance to the arcs, this was done as an extra check that our simulations correspond to the real machine. As in earlier such measurements we find that, on the North side, to get good agreement we need to assume that the compressor voltage readout is low[6], here about 7%. With this adjustment, we find good agreement. An example result of this measurement, compared with simulations, is shown in Fig. 3.

4 RESULTS

In Fig. 4 (top) we show, for $V_c = 37.2$ MV and $\phi = -5.6°$, the measured orbit change (with respect to a long-bunch reference orbit) along the North arc. The bottom frame compares the accumulated energy change deduced from this orbit measurement with the calculated energy change due to the wakefields, taking into account the bunch length evolution. Fig. 4, in addition, shows the calculated contribution to the energy change of the RW and the G wakes, as well as the progression of z_{FWHM}. Note that $z_{FWHM}/2.355$ becomes less than 50 μm near $s = 500$ m. Two more cases are displayed in Fig. 5 (orbits not shown), where the compressor voltage and linac phase were chosen to produce (top) a short bunch near the arc end (entrance to FF) and then (bottom) a short bunch near the reverse bend section ($s \approx 400$ m).

The slopes of the energy change curves of the above two figures give locally the strength of the wakefield effect. For

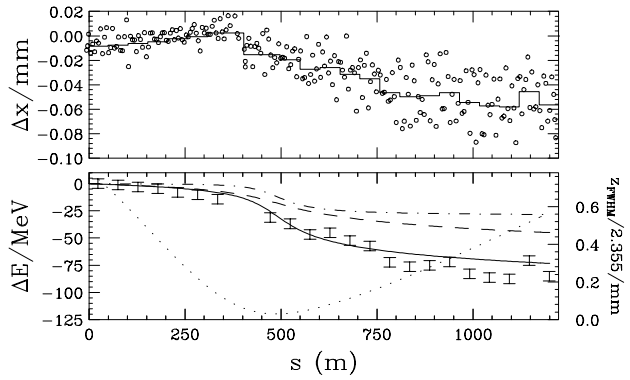

Figure 4: (Top) measured orbit shift for parameters of Fig. 2; (bottom) energy change along arc deduced from top picture, compared with prediction based on calculated wakefields and simulated bunch lengths (*dot-dash*: RW, *dash*: G, *solid*: total, *dots*: bunch length).

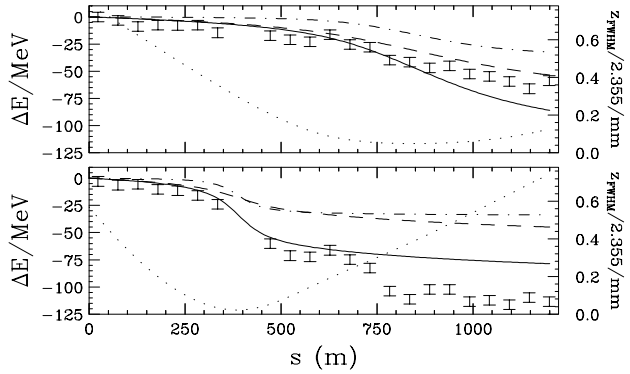

Figure 5: Same plots as in Fig. 4 but: (top) $V_c = 37.2$ MV, $\phi = -11.6°$, and (bottom) $V_c = 34.5$ MV, $\phi = -8.6°$.

all three examples the calculations and the measurements agree well, nearly to within the statistical errors of the measurements, but for two clear exceptions. One exception, apparent in all three examples, is an anomalous energy loss at $s \approx 750$ m. This is especially clear in the case at bottom of Fig. 5, which has the largest net energy loss. In the arcs the absolute orbit is not well known, and this anomaly could be due, for example, to the beam passing closely by a vacuum chamber wall in this region where several corroded vacuum chambers were recently replaced. The other significant disagreement in energy change between the measurement and the calculation is the case at the top of Fig. 5, in the region $s > 850$ m. For this example the bunch length in this part of the arcs is extremely sensitive to the incoming beam parameters, and a slight error may account for the discrepancy. Finally, the measured and calculated average energy loss in the North arc, for several parameter combinations, are given in Table 1.

Since simulations and measurements of energy loss in the arcs are in reasonable agreement, we may assume that the calculated bunch length in the FF is correct. Following the same approach as for the arcs, we can look for a variation of energy loss with bunch length in the FF. Here,

V_c [MV]	$-\phi$ [°]	$-\Delta E_c$ [MeV]	$-\Delta E_m$ [MeV]
34.5	8.6	101	136 ± 4
37.2	5.6	93	102 ± 4
37.2	8.6		79 ± 4
37.2	11.6	82	66 ± 4
40.5	8.6		7 ± 4
42.0	8.6		2 ± 4

Table 1: Calculated (ΔE_c) and measured (ΔE_m) average energy change in the North arc for different settings of compressor voltage, V_c, and linac phase, ϕ.

FF σ_z [μm]	$-\Delta E_c$ [MeV]	$-\Delta E_m$ [MeV]
130	6.2	7.1 ± 0.5
280	2.9	3.9 ± 0.5
570	1.4	0.7 ± 0.5

Table 2: Calculated (ΔE_c) and measured (ΔE_m) average energy change between North and South CCS for different FF bunch lengths.

energy changes can be inferred easily from the orbit at the high-dispersion points ($\eta_x \approx 230$ mm) in the chromatic correction sections (CCSs) on either side of the IP. In the FF there are 26 collimators surrounding the IP and many transitions in beam pipe radius, at each of which a short bunch radiates energy due to the geometric wakefield. The loss is inversely proportional to bunch length[7]. The calculated and measured energy loss for different bunch lengths between the two CCSs is summarized in Table 2. We see that there is reasonable agreement between the results.

5 CONCLUSION AND DISCUSSION

The wakefield-induced energy loss in the North arc has been measured, and for the examples that we have studied the results agree with calculations to within 10–20%; the results are consistent even for calculated bunch lengths approaching 50 μm. Also, there are indications in our data of an anomalous wakefield effect at $s \approx 750$ m, which may be attributable to a large, unconfirmed orbit excursion there.

In the future, a more refined analysis, one accounting for the non-Gaussian bunch distribution, may give more accurate results, particularly in the very short bunch regions. In addition, the energy losses along the South arc should also be measured. With its unshielded bellows we would expect the geometric wakefield effect to be 50% larger.

6 REFERENCES

[1] D. Brandt *et al.*, Proc. of PAC95 Dallas, p. 570 (1995).

[2] A. Chao, "Physics of Collective Beam Instabilities in High Energy Accelerators", John Wiley (1993).

[3] The MAFIA Collaboration, "User Guide", CST GmbH.

[4] K.L.F. Bane, SLAC/AP-80 (1990).

[5] R. Holtzapple, SLAC-R-0487 (PhD Thesis), 1996.

[6] K.L.F. Bane, *et al*, PAC97, Vancouver (1997).

[7] F. Zimmermann, *et al*, EPAC96, Sitges (1996).